Cell, Vol. 99, 301–312, October 29, 1999, Copyright ©1999 by Cell Press

Vascular Endothelial Cell Adherens Junction Assembly and Morphogenesis Induced by Sphingosine-1-Phosphate

Menq-Jer Lee, Shobha Thangada, Kevin P. Claffey, Nicolas Ancellin, Catherine H. Liu, Michael Kluk, Mario Volpi, Ramadan I. Sha'afi, and Timothy Hla*
Center for Vascular Biology
Department of Physiology
University of Connecticut Health Center
Farmington, Connecticut 06030-3501

Summary

Vascular endothelial cells undergo morphogenesis into capillary networks in response to angiogenic factors. We show here that sphingosine-1-phosphate (SPP), a platelet-derived bioactive lipid, activates the EDG-1 and -3 subtypes of G protein–coupled receptors on endothelial cells to regulate angiogenesis. SPP induces the G_i/mitogen-activated protein kinase/cell survival pathway and the small GTPase Rho- and Rac-coupled adherens junction assembly. Both EDG-1- and EDG-3-regulated signaling pathways are required for endothelial cell morphogenesis into capillary-like networks. Indeed, SPP synergized with polypeptide angiogenic growth factors in the formation of mature neovessels in vivo. These data define SPP as a novel regulator of angiogenesis.

Introduction

Angiogenesis, the process of new blood vessel formation, is important in embryonic development as well as physiological events. Dysregulated angiogenesis is involved in various pathological conditions, for example, solid tumor growth, rheumatoid arthritis, and diabetic retinopathy (Folkman, 1995). Angiogenesis is initiated by vascular endothelial cells and involves their orderly proliferation, migration, and morphogenesis into new capillary networks. Such events are precisely regulated by soluble growth factors as well as extracellular matrix–derived signals (Folkman, 1995; Bader et al., 1998; Eliceiri and Cheresh, 1999). The balance between positive (angiogenic) and negative (anti-angiogenic) factors in vivo may be important for the control of angiogenesis (Iruela-Arispe and Dvorak, 1997; O'Reilly et al., 1997).

Folkman and Haudenschild showed that stimulation of isolated endothelial cells with tumor-conditioned medium induces the formation of capillary-like networks (Folkman and Haudenschild, 1980). These early studies suggested that the endothelial cells are capable of expressing the genetic machinery required to form a capillary network when appropriately stimulated. Thus, cultured endothelial cells have become a widely used model system to elucidate the mechanisms of angiogenesis. Treatment of endothelial cells grown on three-dimensional collagen or fibrin gels with phorbol 12-myristic 13-acetate (PMA) results in the formation of networks of capillary-like structures (Montesano and Orci, 1985). Angiogenic factors such as VEGF and FGF induce endothelial cell migration, mitogenesis, and survival (Friesel and Maciag, 1995; Ilan et al., 1998; Satake et al., 1998). In addition, VEGF is a potent inducer of vascular permeability, a prerequisite initial event for plasma exudation and fibrin clot formation, a matrix permissive for angiogenesis (Iruela-Arispe and Dvorak, 1997). However, factors and mechanisms that regulate morphogenesis of endothelial cells into capillary-like networks are poorly understood.

The *EDG-1* (*E*ndothelial *D*ifferentiation *G*ene-1) gene, which encodes a G protein–coupled receptor (GPCR), is rapidly induced by PMA in human umbilical vein endothelial cells (HUVEC) (Hla and Maciag, 1990). Several other GPCRs related in primary sequence to EDG-1 were isolated from different laboratories, including EDG-2/VZG-1 (Hecht et al., 1996), EDG-3 (Yamaguchi et al., 1996), EDG-4 (An et al., 1998), and EDG-5 (Okazaki et al., 1993). EDG-1, EDG-3, and EDG-5 are high-affinity receptors for the platelet-derived bioactive lipid sphingosine-1-phosphate (SPP) (Yatomi et al., 1997; Lee et al., 1998; Ancellin and Hla, 1999), whereas EDG-2 and EDG-4 are lysophosphatidic acid (LPA) receptors (Hecht et al., 1996; An et al., 1998). The EDG-1 family of receptors are developmentally regulated and differ in tissue distribution (Hecht et al., 1996; Liu and Hla, 1997). Also, EDG-1 couples to G_i (Lee et al., 1996) but not the G_q protein; whereas EDG-3 potently activated G_q and G_{13} polypeptides (Ancellin and Hla, 1999; Windh et al., 1999). EDG-5 also couples to G_q, albeit less effectively than EDG-3, although it is capable of activating G_{13} (Ancellin and Hla, 1999; Windh et al., 1999). Thus, EDG-1, -3, and -5 are SPP receptor subtypes that couple to different signaling pathways.

SPP is synthesized intracellularly by the sequential actions of sphingomyelinase, ceramidase, and sphingosine kinase (Spiegel and Merril, 1996). SPP, like its structural relative LPA, is responsible for much of the lipid-derived biological activities of serum—such as proliferation, survival, stress fiber and focal adhesion plaque formation, fibronectin matrix assembly, cell rounding, and cell migration (reviewed in Hla et al., 1999). Controversy exists as to whether SPP acts as an extracellular mediator or an intracellular second messenger (Hla et al., 1999). Although these roles need not be mutually exclusive, it is important to define precisely which receptor/effector pathway is important for specific biological actions of SPP.

In this study, we describe a novel extracellular function of SPP as an angiogenic modulator.

Results

EDG-1 and -3 Are Functional SPP Receptor Subtypes in Endothelial Cells

Northern blot analysis of HUVEC poly(A)$^+$ RNA showed that *EDG-1* was abundantly expressed, the *EDG-3* tran-

*To whom correspondence should be addressed (e-mail: hla@sun.uchc.edu).

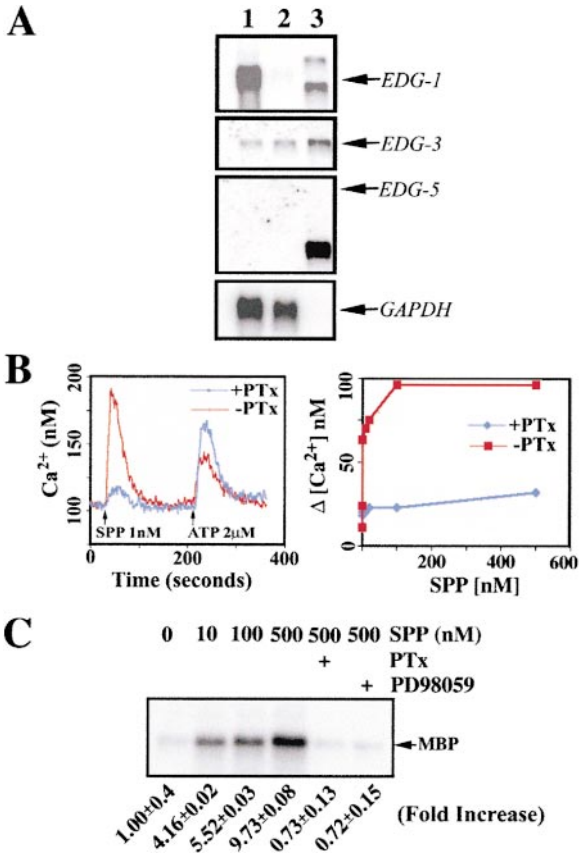

Figure 1. Expression of EDG-1 and EDG-3 in Endothelial Cells

(A) Poly(A)$^+$ RNA from HUVEC (lane 1) and HEK293 (lane 2) were probed with *EDG-1*, *-3*, *-5*, or *GAPDH* cDNAs. Positive control (lane 3), in vitro transcripts for EDG-1, -3, and -5.

(B) SPP-induced intracellular calcium. HUVEC were loaded with Indo-1, stimulated with different doses of SPP, and Ca^{2+} (in nM) was quantitated. Some cells were pretreated with PTx (500 ng/ml) for 16 hr. $\Delta[Ca^{2+}]$ represents the difference in intracellular free Ca^{2+}.

(C) SPP induces G_i-dependent MAP kinase activation. Endothelial cells were stimulated with SPP for 10 min and ERK-2 kinase activity was measured by an immune complex kinase assay as described. Some cells were pretreated with PTx (200 ng/ml) or PD98059 (10 μM) for 2 hr prior to stimulation.

script was expressed at a much lower level and the *EDG-5* mRNA was undetectable (Figure 1A). EDG-1 expression was estimated to be 16-fold more abundant than EDG-3. In contrast, EDG-3 is the predominant SPP receptor isotype in human embryonic kidney (HEK)293 cells.

We next tested, by sensitive functional assays, the presence of G_i- and G_q-coupled SPP receptors in HUVEC. As shown in Figure 1B, SPP induced a robust calcium response in endothelial cells, which was inhibited approximately 90% by pertussis toxin, whereas the G_q-coupled ATP receptor response was not pertussis toxin sensitive. These data suggest that EDG-1, a G_i-coupled SPP receptor, is responsible for the majority of SPP-induced calcium responses in HUVEC. The pertussis toxin–resistant component may be due to the activity of EDG-3. Secondly, we utilized the SPP-induced extracellular signal–activated kinase (ERK) activation assay. As shown in Figure 1C, SPP (10–500 nM) activated ERK activity in a dose-dependent manner in HUVEC. This response was inhibited completely by pretreating cells with pertussis toxin and PD98059, indicating that this activity is dependent on the G_i protein and MAP kinase kinase. Complete inhibition by pertussis toxin suggests that most of the SPP effects on MAP kinase are mediated by EDG-1.

Regulation of Adherens Junction Assembly by SPP

Treatment of endothelial cells with SPP for 30 min resulted in dramatic increase in actin stress fibers and cortical actin structures in endothelial cells (see Supplemental Data below). These effects are mediated by the plasma membrane receptors because intracellular microinjection of SPP induced neither stress fibers nor cortical actin (see Supplemental Data).

The formation of stress fibers and cortical actin in 3T3 fibroblasts is dependent on the activity of Rho and Rac small GTPases, respectively (Ridley et al., 1992; Hall, 1998). Intracellular microinjection of the C3 exoenzyme, a specific inhibitor of Rho abolished the SPP-induced stress fibers but not the cortical actin. Microinjection of dominant-negative Rac protein (N17Rac) completely inhibited the formation of both stress fibers and cortical actin. Pertussis toxin did not inhibit either of the actin changes in endothelial cells (see Supplemental Data). These data suggest that the extracellular action of SPP via a non-G_i-dependent pathway transduces signals through the Rac and Rho small GTPases to regulate the cytoskeletal architecture of endothelial cells. Furthermore, similar to the findings in fibroblasts (Ridley et al., 1992; Hall, 1998), Rac appears to act upstream of Rho in the induction of endothelial cell cytoskeletal changes.

We showed previously that SPP induces morphogenetic differentiation and upregulates P-cadherin-based adherens junctions in EDG-1-transfected HEK293 cells (Lee et al., 1998). Thus, we investigated the effect of SPP on cell–cell junctions in endothelial cells. When HUVEC were treated with SPP, VE-cadherin, α-, β-, and γ-catenin localization at cell–cell junctions was dramatically increased within 1 hr (Figure 2A and data not shown). Confocal immunofluorescence microscopy indicates that SPP treatment increased the localization of VE-cadherin (Figures 2A and 3C) into discontinuous structures at cell–cell contact regions, suggesting that SPP induces the formation of adherens junctions. Treatment with related lipids (sphingosine, sphingomyelin, ceramide, ceramide-1-phosphate) that do not interact with SPP receptors had no effect (data not shown). Also, direct microinjection of SPP (ranging from 500 nM to 500 μM) into the cytoplasm did not increase the immunoreactivity of VE-cadherin and catenins at cell–cell junctions (see Supplemental Data).

Formation of mature adherens junctions requires homophilic binding of intercellular cadherins, association with cytoplasmic polypeptides, and attachment to the cytoskeleton, which ultimately results in the partitioning of cadherin molecules into the detergent-insoluble fraction (Yap et al., 1997). Fractionation of HUVEC cell lysates showed that SPP-induced, in a dose- and

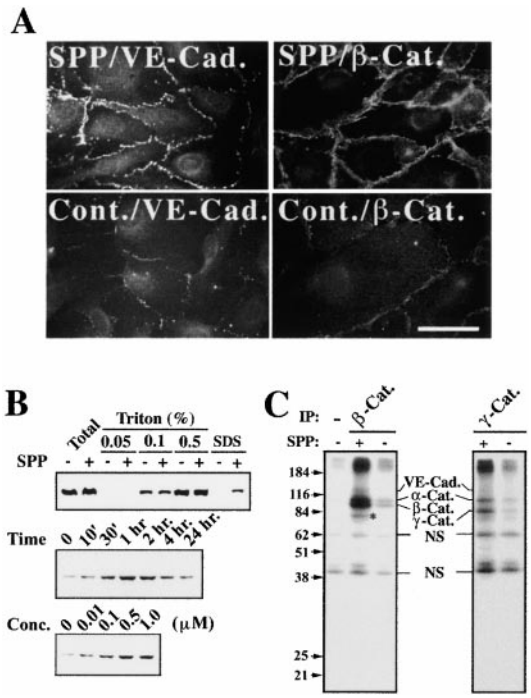

Figure 2. SPP Induces Adherens Junction Assembly in Endothelial Cells

(A) Recently confluent HUVEC cells were treated with (SPP, 500 nM) or without (Cont.) for 1 hr, and immunofluorescence analysis of VE-cadherin and β-catenin was done. Data are representative of at least six experiments. Scale bar = 13.4 μm.

(B) SPP induces Triton-X-100 insolubility of VE-cadherin. Unstimulated HUVEC cells (−) or cells stimulated with 500 nM of SPP for 1 hr (+) were sequentially fractionated with Triton X-100 (0.05%, 0.1%, 0.5%). The insoluble lysates were further extracted with 1% Triton X-100 plus 1% SDS (SDS) at 95°C for 10 min. Equal amounts of protein extracts were probed with anti-VE-cadherin antibody (upper panel). (Middle panel) HUVEC cells were stimulated with 500 nM of SPP for indicated times, Triton X-100–insoluble pellets were prepared and probed for VE-cadherin. (Lower panel) HUVEC cells were treated for 1 hr with indicated concentration of SPP. Triton X-100–resistant VE-cadherin levels were determined.

(C) SPP induces adherens junctional complexes in detergent-insoluble fractions. HUVEC cells were labeled with [^{35}S]-methionine and treated or not with 500 nM SPP. Protein complexes in the insoluble fractions were cross-linked by DSP and immunoprecipitated with respective antibodies as described. (*), an unidentified polypeptide with apparent molecular mass of 80 kDa. NS, polypeptides bound to protein A beads nonspecifically.

time-dependent manner, an increase in the amount of VE-cadherin in the Triton X-100 insoluble fraction; however, the overall level of protein was not altered (Figure 2B). Consistent with the immunofluorescence data, the increase of VE-cadherin in Triton X-100 insoluble fractions peaked at 1–2 hr following SPP treatment.

To directly show that SPP signaling in endothelial cells regulates adherens junction assembly, a coimmunoprecipitation experiment was conducted. As shown in Figure 2C, SPP significantly increased the α-catenin and VE-cadherin polypeptides in the γ- and β-catenin immunoprecipitates. In agreement with previous findings (Hinck et al., 1994), β-catenin and γ-catenin are found in a mutually exclusive manner in adherens junctional complexes.

Requirement for Rac and Rho GTPases in SPP-Induced Adherens Junction Assembly

Next, we examined the subcellular localization of Rac and Rho in HUVEC before and after SPP treatment. Interestingly, treatment with SPP for 10–30 min resulted in significant redistribution of Rac to the cell–cell contact areas, whereas subcellular localization of Rho was not altered (Figure 3A). Tiam1, a guanine nucleotide exchange factor specific for Rac (Michiels et al., 1995), was also translocated to cell–cell contact areas (Figure 3A). Double immunostaining exhibited an overlapping pattern between Tiam1 and β-catenin after SPP treatment.

To determine if Rho and Rac small GTPases are required for SPP-induced adherens junction assembly, C3 exoenzyme and dominant-negative N17Rac polypeptide were microinjected into HUVEC cells. As shown in Figures 3B and 3C, microinjection of C3 and N17Rac dramatically diminished SPP-induced VE-cadherin immunoreactivity at cell–cell junctions. Similar results were observed for β-catenin immunoreactivity (see Supplemental Data). Neither the injection of FITC-mouse IgG nor the inactivation of the heterotrimeric G_i protein by treatment or microinjection of pertussis toxin inhibited VE-cadherin and β-catenin localization at cell–cell junctions (data not shown). These data suggest that SPP-induced Rho and Rac activation is required for adherens junction assembly in HUVEC.

Requirement for EDG-1 and EDG-3 in SPP-Induced Cytoskeletal Changes and Adherens Junction Assembly

We next determined the involvement of the EDG-1 and -3 subtypes of SPP receptors in the assembly of adherens junctions. For this, antisense phosphothioate oligonucleotides (PTO), which are designed to bind to the translational initiation site on the mRNA and thus block the expression of EDG-1 and -3 receptors were developed. As shown in Figure 4A, coinjection of EDG-1 antisense PTO with the *EDG-1* cRNA into *Xenopus* oocytes resulted in profound inhibition of EDG-1 expression, as determined by suppression of SPP-induced calcium rises (Ancellin and Hla, 1999). EDG-3 antisense PTO did not inhibit the *EDG-1* cRNA expression, indicating specificity. Likewise, EDG-3 antisense PTO only inhibited the respective cRNA for EDG-3. These data suggest that the EDG-1 and -3 PTOs are specific inhibitors of respective receptor expression. These reagents were microinjected into the cytoplasm of HUVEC to block the expression of EDG-1 and -3 receptors, and SPP-induced VE-cadherin assembly into cell-cell junctions was analyzed. As shown in Figure 4B and Table 1, both EDG-1 and -3 antisense PTOs inhibited the SPP-induced VE-cadherin localization at cell–cell junctions. In contrast, neither the complementary nor the scrambled sequence of EDG-1 and -3 oligonucleotides inhibited VE-cadherin assembly significantly. Furthermore, antisense EDG-1 PTO attenuated the formation of cortical actin structures in HUVEC, which are known to be induced by the Rac pathway (Figure 4C). In contrast, formation of stress

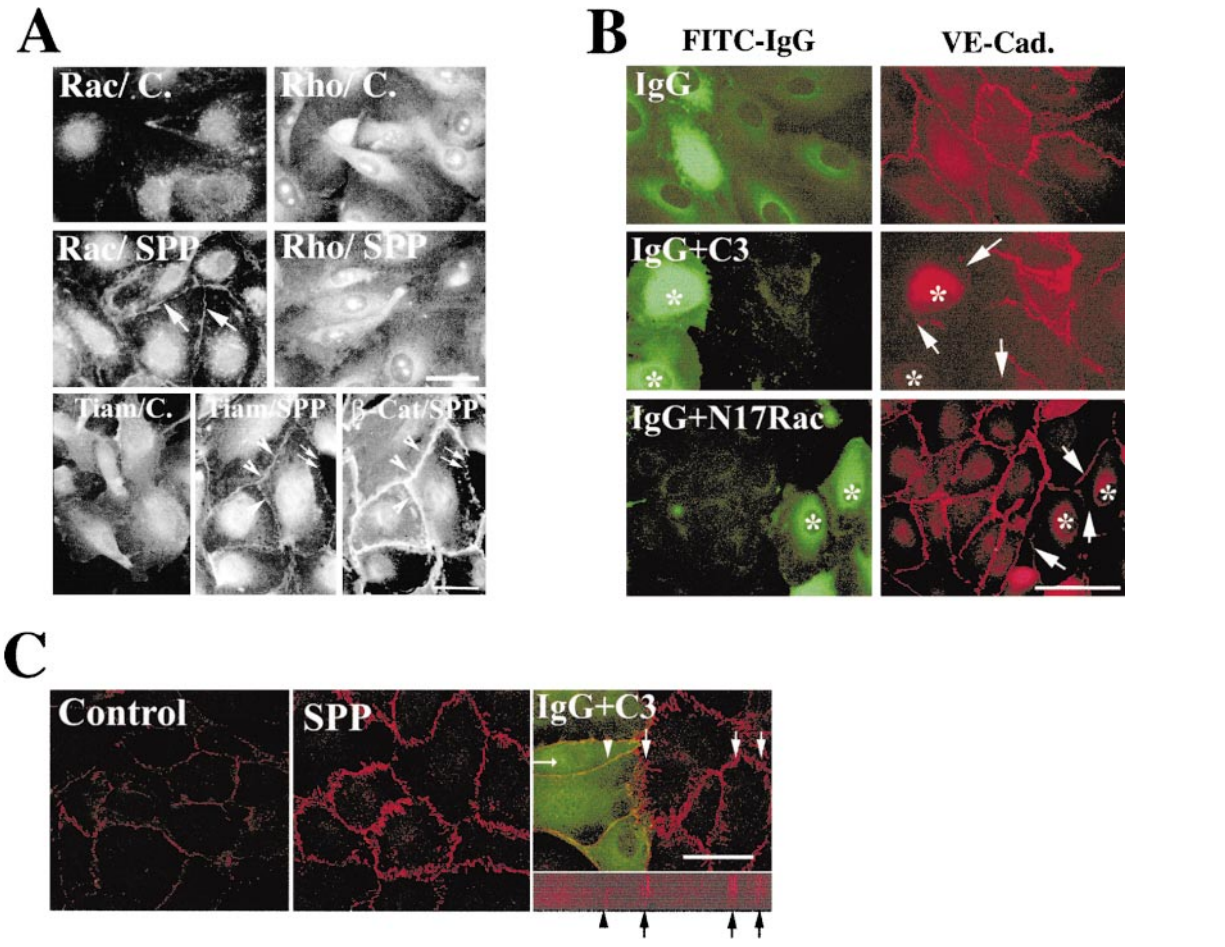

Figure 3. SPP-Induced Adherens Junction Assembly Requires Rho and Rac Small GTPases

(A) SPP induces the translocation of Rac and Tiam1 to cell–cell contact sites. HUVEC cells were stimulated with 500 nM of SPP for 30 min, immunostained with Rac or Rho antibodies. Scale bar, upper panels = 8.7 μm. In the lower panels, cells were labeled with Tiam1 and β-catenin antibodies, and then stained with FITC-goat anti-rabbit and TRITC-sheep anti-mouse antibodies, respectively. SPP induces both Tiam1 and β-catenin translocation to cell–cell contact sites (indicated by arrowheads), but not the isolated cell edges (arrows). Scale bar, lower panels = 7.7 μm; C., control.

(B) SPP-induced VE-cadherin translocation to cell–cell junctions requires Rho and Rac GTPases. HUVEC were microinjected with FITC-IgG alone (first row), FITC-IgG together with C3 exoenzyme (second row), or N17Rac (third row). Following stimulation with SPP, cells were stained with anti-VE-cadherin. Note that injection of C3 and N17Rac diminished the SPP-induced VE-cadherin immunoreactivity at cell–cell contact areas (arrows). Scale bar = 20 μm.

(C) confocal images of anti-VE-cadherin staining in unstimulated (left) or SPP-stimulated (middle) HUVEC. When cells were injected with FITC-IgG plus C3 exotoxin and stained with anti-VE-cadherin, superimposed confocal image (right) shows that SPP-induced zigzag-like staining pattern was reduced to a smooth plasma membrane staining pattern by C3 treatment (green cells). Lower inset shows the Z section of the confocal image. Note that strong VE-cadherin staining was observed in the apical region of cell–cell junctions in uninjected cells (vertical arrows), whereas only a weakly stained basolateral smooth line was observed in C3-injected cells (vertical arrowhead). The position of Z section is indicated by a horizontal arrow. Scale bar = 11.25 μm.

fibers was specifically inhibited by antisense EDG-3 PTO. These data support the notion that induction of Rac pathway by EDG-1 and Rho pathway by EDG-3 are necessary for the SPP-induced adherens junction assembly.

SPP-Induced Morphogenesis of Endothelial Cells: Requirement for G_i-Dependent Cell Survival and Rho/Rac-Dependent Adherens Junction Assembly

We next investigated the effect of SPP on morphogenetic differentiation of endothelial cells. We used matrigel, which is known to promote the morphogenesis on HUVEC into capillary-like networks (Passaniti et al., 1992). As shown in Figure 5, SPP, in a dose-dependent manner, promoted HUVEC morphogenesis, whereas other lipid analogs ceramide-1-phosphate and sphingomyelin were inactive. The maximal effects achieved by 1 μM SPP were indistinguishable from the positive control medium which contained FBS. Also, SPP, ranging from 100 nM to 1 μM, induced morphogenesis of bovine microvascular endothelial cells (data not shown).

Inactivation of the heterotrimeric G_i protein by pertussis toxin inhibited the SPP-induced morphogenesis sug-

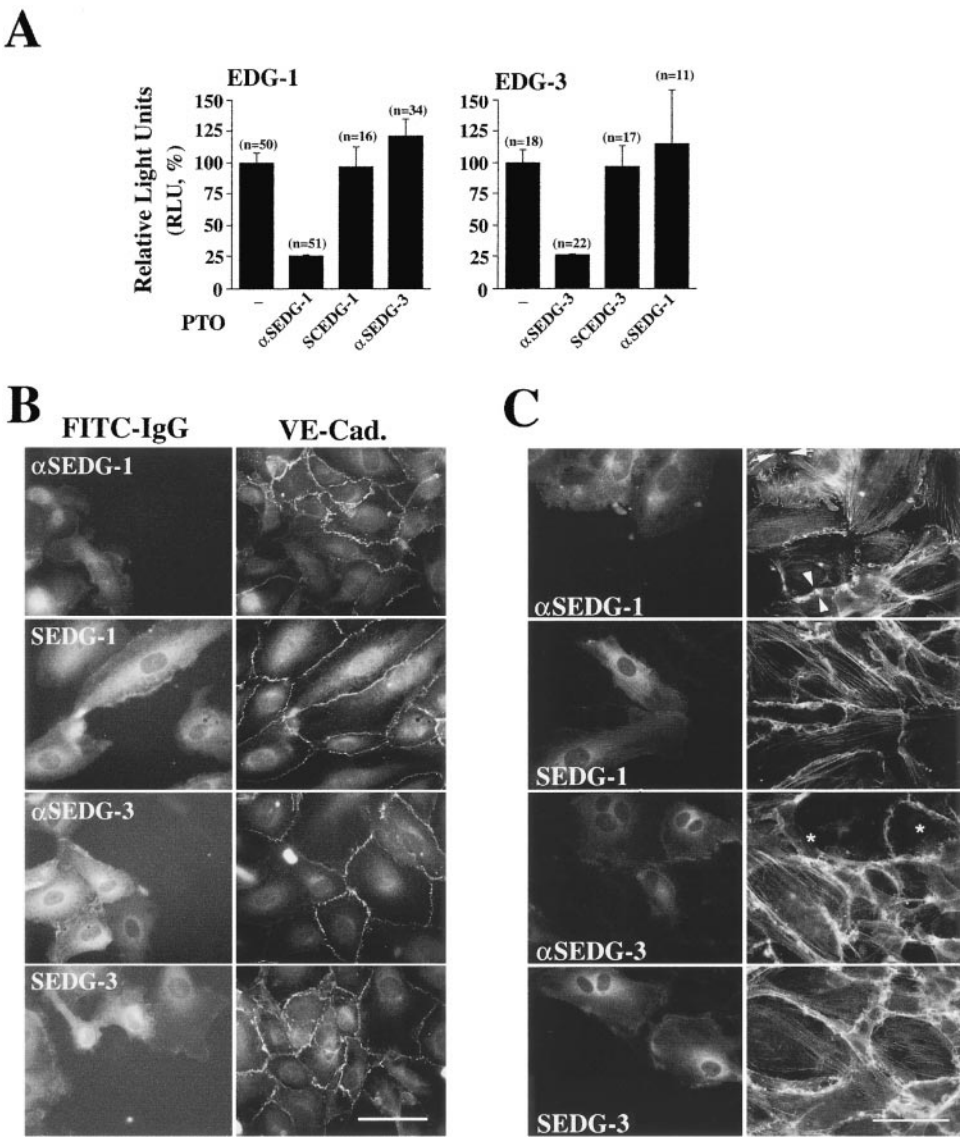

Figure 4. EDG-1 and EDG-3 Mediate SPP-Induced Cytoskeletal Reorganization and Adherens Junction Assembly

(A) Characterization of the efficacy and specificity of EDG-1 and EDG-3 PTOs. *Xenopus* oocytes were injected with in vitro transcribed RNA and indicated PTO, and Ca^{2+} rises induced by SPP were performed as described. n = number of oocytes injected.

(B) EDG-1 and EDG-3 expression is required for SPP-induced adherens junction assembly. HUVEC were microinjected with antisense (αs) or sense (s) PTO (20 μM in the micropipette) for EDG-1 and EDG-3 as described. Eighteen to twenty-four hours thereafter, cells were stimulated with 0.5 μM SPP for 1 hr, fixed, and VE-cadherin localization was determined by immunofluorescence microscopy. FITC-IgG column indicates the microinjected cells, and VE-Cad panels indicate the signal for VE-cadherin in the same microscopic field. Scale bar = 16 μm.

(C) EDG-1 and EDG-3 regulation of SPP-induced cytoskeletal dynamics. HUVEC were microinjected with EDG-1 and -3 PTO and actin cytoskeleton was labeled with TRITC-phalloidin as described. Microinjected cells are marked with the FITC-IgG (left column). Note that the EDG-1 antisense PTO specifically inhibited cortical actin (arrows indicate injected cells; arrowheads, uninjected cells) whereas the EDG-3 PTO blocked stress fiber formation (asterisks indicate injected cells). Scale bar = 17 μm.

gesting that a G_i-dependent SPP signaling pathway is essential (Figure 5B). It is known that a critical function of angiogenic factors is to promote endothelial cell survival (Ilan et al., 1998; Satake et al., 1998). Indeed, SPP, in a dose-dependent manner (10–500 nM), significantly protected cells from apoptosis induced by C_2-ceramide (Figures 5E and 5F). This effect was also seen when growth factor withdrawal and 15-deoxy-$\Delta^{12,14}$ prostaglandin J_2 were used as apoptotic stimuli (data not shown). This cytoprotective effect of SPP is completely inhibited in the presence of pertussis toxin and PD98059 (Figure 5F). Also, antisense EDG-1 PTO treatment reduced the ability of SPP to block ceramide-induced apoptosis (44% ± 4%) whereas sense EDG-1 PTO or antisense EDG-3 or EDG-5 PTO did not have significant effects (<5%). These data strongly suggest that EDG-1/G_i/ERK pathway mediates SPP-induced endothelial cell survival.

The Rho inhibitor C3 exoenzyme abolished SPP-induced morphogenesis of endothelial cells (Figure 5B).

Table 1. SPP-Mediated Cytoskeletal Changes and Adherens Junction Assembly Requires EDG-1 and EDG-3 Expression

Treatments		Cortical Actin (% of cells inhibited)	Stress Fiber (% of cells inhibited)	VE-Cadherin (% of cells inhibited)
αSEDG-1	(40 μM)	79 ± 12 (n = 90)*	36 ± 15 (n = 90)	89 ± 9 (n = 120)*
αSEDG-1	(20 μM)	64 ± 7 (n = 90)*	17 ± 8 (n = 90)	72 ± 11 (n = 200)*
αSEDG-1	(10 μM)	ND	11 ± 10 (n = 40)	67 ± 14 (n = 70)*
SEDG-1	(40 μM)	25 ± 7 (n = 70)	21 ± 13 (n = 70)	21 ± 11 (n = 90)
SEDG-1	(20 μM)	ND	13 ± 6 (n = 30)	16 ± 13 (n = 70)
SCEDG-1	(20 μM)	13 ± 6 (n = 200)	14 ± 5 (n = 200)	9 ± 7 (n = 260)
αSEDG-3	(20 μM)	4 ± 2 (n = 40)	66 ± 9 (n = 40)*	53 ± 10 (n = 170)*
SEDG-3	(20 μM)	8 ± 6 (n = 140)	12 ± 8 (n = 140)	8 ± 5 (n = 150)
αSEDG-5	(20 μM)	12 ± 7 (n = 230)	13 ± 8 (n = 230)	10 ± 7 (n = 160)
FITC-IgG		12 ± 8 (n = 220)	11 ± 9 (n = 210)	9 ± 8 (n = 210)

HUVEC cells were injected with indicated PTO. αs = antisense, s = sense, sc = scrambled. The concentration of PTO in the micropipette is indicated in the parentheses. 16–24 hr later, cells were stimulated with SPP (500 nM), fixed, and stained for VE-cadherin and actin. (*) indicates statistical significance ($p < 0.01$, t test) of PTOs treatment versus control (FITC-IgG alone). n = numbers of cells scored. ND, not determined.

We therefore examined the functional relationship between SPP-induced adherens junction assembly and endothelial cell morphogenesis. As shown in Figure 5C, the anti-VE-cadherin blocking monoclonal antibody (Bach et al., 1998) inhibited SPP-induced morphogenesis dose-dependently. Moreover, as shown in Figure 5D, EDG-1 and EDG-3 antisense PTO attenuated SPP-induced HUVEC morphogenesis. Coadministration of both PTOs reduced morphogenesis in an additive manner. In contrast, similar doses of EDG-1, -3 scrambled or sense sequences or the EDG-5 antisense PTO failed to block the SPP-induced endothelial cell morphogenesis (Figure 5D).

These data indicate that SPP activation of endothelial cells stimulates two distinct signaling pathways regulated by EDG-1 and -3 receptors: namely, EDG-1/G_i-mediated endothelial cell survival and Rho-/Rac-mediated VE-cadherin assembly into adherens junctions. Rho appears to be induced by EDG-3 and Rac by EDG-1 signaling. Both of these receptor-regulated signaling pathways are important for endothelial cell morphogenesis into capillary-like networks. This is schematically represented in Figure 7.

Effects of SPP on Growth Factor–Induced Angiogenesis In Vivo

To determine if SPP regulates angiogenesis in vivo, we utilized the matrigel implant model of subcutaneous angiogenesis in athymic mice (Passaniti et al., 1992). As shown in Figure 6, SPP dramatically enhanced FGF-2-induced angiogenesis; vascular density and the appearance of mature vascular structures were greatly increased by SPP (Figures 6A and 6B). Supplementation of FGF-2 with sphingosine did not potentiate angiogenesis. Interestingly, SPP also potentiated VEGF-induced angiogenesis and antisense PTO of EDG-1 and EDG-3 attenuated the formation of mature neovessels in vivo (Figure 6C). Transmission EM analysis indicated that neovessels with well-developed adherens junctions were increased by the FGF-2 and SPP treatment (Figure 6D). In addition, SPP treatment induced neovessel maturation, as evident by the appearance of basement membrane-like structures. These data provide an in vivo correlate of our in vitro findings that SPP signaling via the EDG-1 and EDG-3 receptors induce morphogenetic differentiation of endothelial cells.

Discussion

HUVEC express EDG-1 abundantly and EDG-3 at low levels. Previous studies have shown that EDG-1 binds to the heterotrimeric G_i protein and induces ERK activity (Lee et al., 1996). However, EDG-1 is not capable of inducing G_q-dependent responses whereas EDG-3 is efficiently coupled to G_q and G_{13} (Ancellin and Hla, 1999; Windh et al., 1999). Indeed, nanomolar concentrations of extracellular SPP induced intracellular calcium rises as well as ERK activation, and the majority of those effects are inhibited by pertussis toxin, a specific inhibitor of the G_i pathway. It is well established that both intracellular calcium rises and ERK activation can be induced by both G_i as well as G_q pathways (Exton, 1997). These data suggest that the majority of calcium changes and ERK activation are mediated by the G_i-coupled SPP receptor EDG-1.

Bioactive lipids such as SPP and LPA regulate cytoskeletal architecture by signaling through the Rho family of GTPases (Ridley et al., 1992; Nobes and Hall, 1995; Postma et al., 1996; Hall, 1998). We show that in endothelial cells SPP acts as an extracellular mediator to induce actin stress fibers and cortical actin. Induction of stress fibers required the activity of Rho whereas dominant-negative Rac inhibited both stress fibers and cortical actin assembly. As expected, SPP effects on the cytoskeleton are not inhibited by pertussis toxin. These data suggest that SPP interaction with HUVEC regulates Rho and Rac activity by a G_i-independent pathway. The question raised by these studies is whether Rho and Rac effects are mediated by EDG-1 or EDG-3 or both.

Significantly, SPP treatment of HUVEC regulates the translocation of Tiam1 (an upstream activator of Rac) and Rac to cell–cell junctions. Furthermore, VE-cadherin and catenin molecules are also translocated to discontinuous structures at cell–cell junctions in response to SPP. Moreover, VE-cadherin partitions into a detergent-insoluble fraction after SPP treatment, suggesting that SPP induces adherens junction assembly in HUVEC. Indeed, immunoprecipitation experiments suggest that detergent insoluble β- and γ-catenin are found associated with other adherens junction proteins and VE-cadherin after SPP treatment. These data indicate that the adherens junctions in endothelial cells are under dynamic control by SPP signaling. In contrast, polypeptide

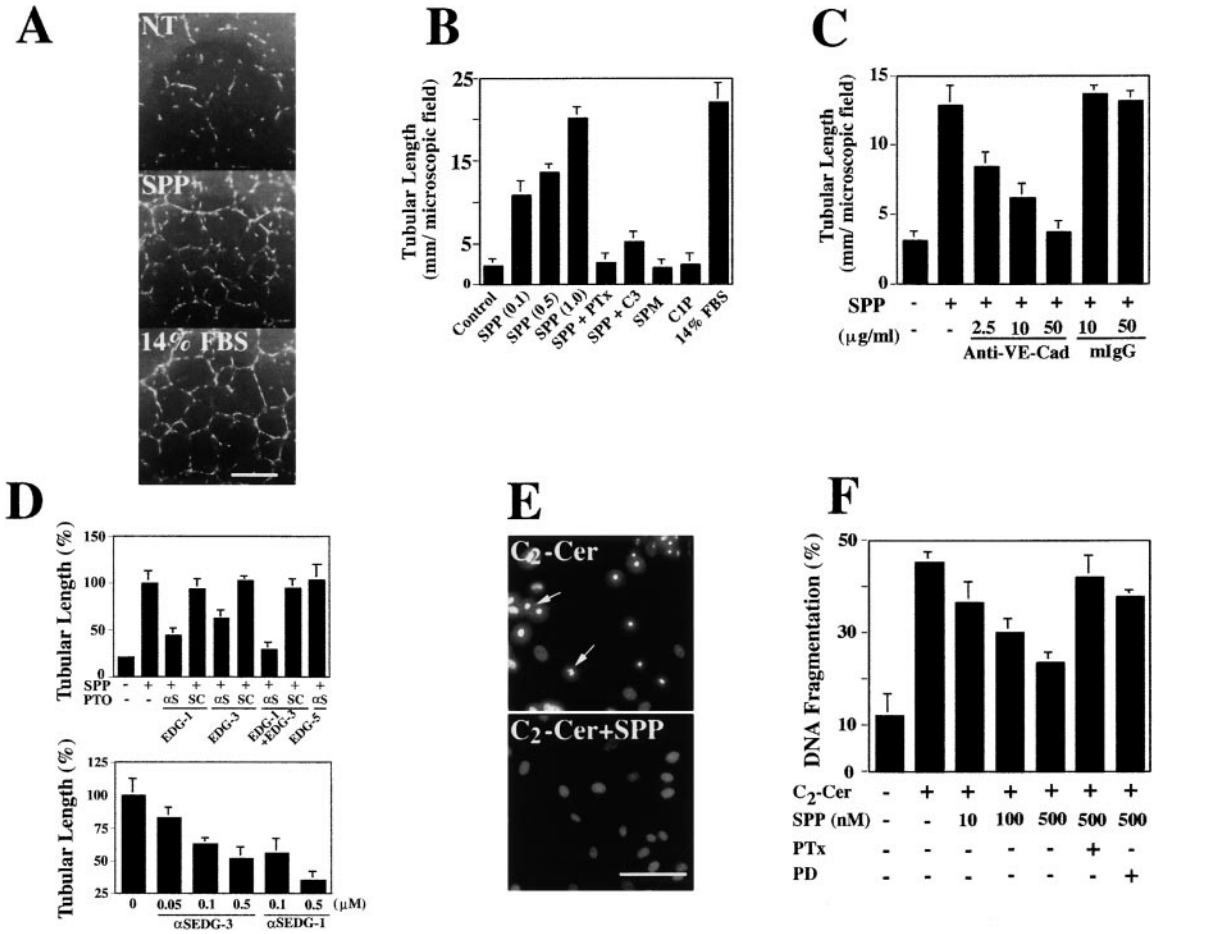

Figure 5. EDG-1 and EDG-3 Mediate SPP-Induced Morphogenesis and Survival of Cultured Endothelial Cells

Morphogenesis on matrigel (A) and quantitative analysis of tubular length (B–D) were done as described. Scale bar = 52 μm. SPP concentrations are indicated in parenthesis (in μM). SPP+PTx, HUVEC were pretreated with pertussis toxin (PTx, 200 ng/ml) for 2 hr, trypsinized, plated onto matrigel, stimulated with 500 nM SPP in the presence of PTx (20 ng/ml). SPP + C3, HUVEC cells were pretreated with C3 exoenzyme (10 μg/ml) for 48 hr, trypsinized, plated onto matrigel, stimulated with 500 nM SPP together with same concentration of C3 exotoxin. SPM, sphingomyelin (1 μM); C1P, C8-ceramide-1-phosphate (1 μM). (C) VE-cadherin is required for SPP-induced morphogenesis. Cultured HUVEC were pretreated with various concentrations of anti-VE-cadherin or irrelevant mouse IgG (mIgG) for 1 hr. Cells were then trypsinized, plated onto matrigel in the presence of same amounts of corresponding antibodies without or with 500 nM of SPP. (D) EDG-1 and -3 PTO inhibit SPP-induced morphogenesis. Individual PTO (0.2 μM in upper panel) was delivered into HUVEC by lipofectin reagent as described. Twenty-four hours later, cells were trypinized, plated onto matrigel in the absense or presence of SPP (500nM) and tubular length was quantitated. (E) HUVEC were treated with C_2-ceramide in the absence (C_2-Cer) or presence (C_2-Cer + SPP) of 500 nM SPP. The apoptotic nuclei (arrows) were identified by staining with the Hoechst dye. Scale bar = 31 μm. (F) HUVEC survival promotion by SPP is dependent on the G_i/MAP kinase pathway. Cells were incubated with [methyl-^{3}H]-thymidine for 24 hr to label DNA, and then washed before exposure to C_2-ceramide in the presence or absence of SPP for 12 hr. SPP+PTx and SPP+PD98059: cells were pretreated with pertussis toxin (200 ng/ml) and PD98059 (10 μM), respectively, for 2 hr prior to the addition of C_2-ceramide and SPP.

cytokines such as VEGF and TNF-α are known to disrupt adherens junctions (Esser et al., 1998; Wojciak-Stothard et al., 1998), a phenomenon which may be responsible for enhanced vascular permeability and increased extravasation of blood-borne cells. Therefore, under physiological conditions in the adult, SPP may promote endothelial cell integrity and functionality.

SPP-stimulated translocation of VE-cadherin and β-catenin to cell–cell junctions requires the activity of Rho and Rac GTPases. Similar to the regulation of actin cytoskeleton, microinjection of SPP into HUVEC cells did not regulate VE-cadherin and β-catenin translocation, suggesting that extracellular action of SPP on plasma membrane receptors is involved. In addition, pertussis toxin treatment did not inhibit VE-cadherin and β-catenin translocation, suggesting that a non-G_i pathway is involved. These data agree with previous findings in epithelial cells and keratinocytes that adherens junction assembly requires the activity of Rho and Rac (Braga et al., 1997; Takaishi et al., 1997). That Tiam1 and Rac colocalize with β-catenin after SPP treatment suggests that they may directly participate in the linkage of cadherin complexes to the cytoskeleton. Mechanistic details of how GPCRs regulate Rho and Rac activity are not well understood. The G_{13} and G_q family of heterotrimeric G proteins have been implicated in Rho activation and stress fiber assembly (Katoh et al.,1998). Alternatively, a recent study has shown that

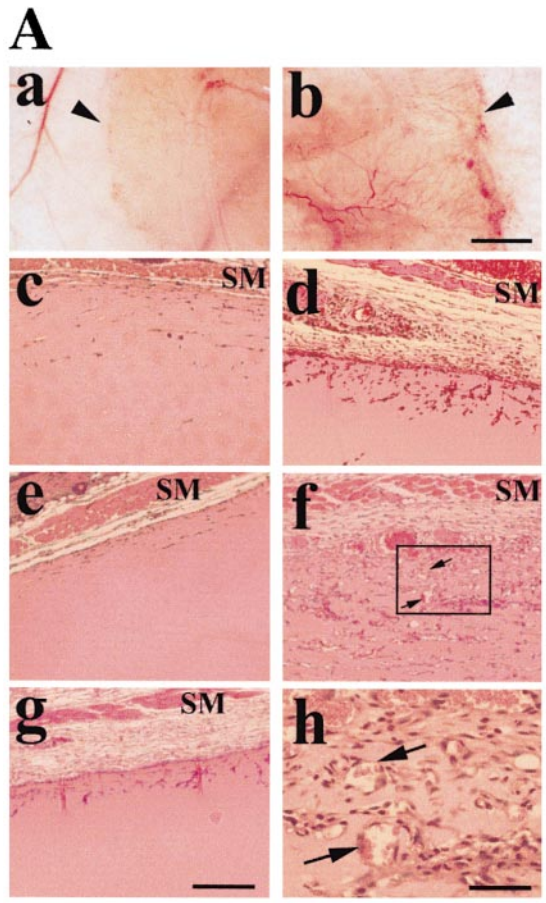

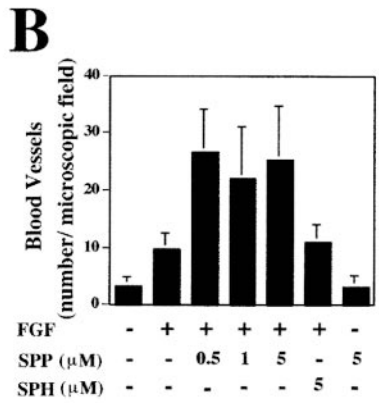

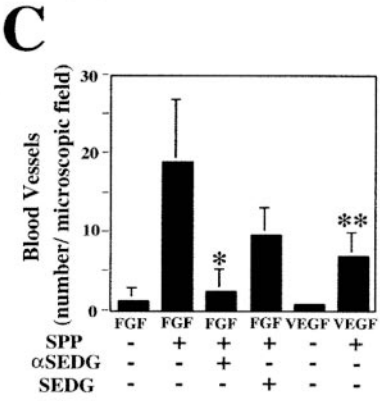

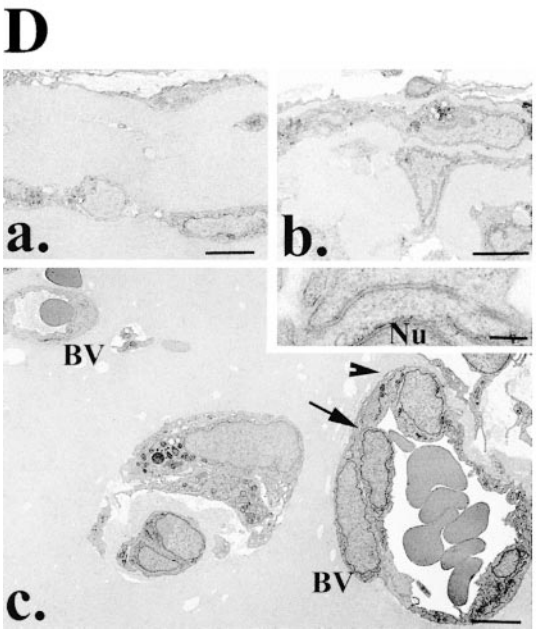

Figure 6. SPP Potentiates FGF-2- and VEGF-Induced Angiogenesis In Vivo

(A) Panels (a) and (b) show the low-power micrograph of angiogenic response in implanted matrigel plugs, whereas (c)–(h) show the histological analysis of sections of matrigel plugs stained with hematoxylin and eosin. (a) and (d), FGF-2 alone; (b), (f), and (h), SPP + FGF-2; (c), vehicle control; (e), SPP alone; and (g), sphingosine (SPH) + FGF. (h) is a high-power view of the boxed area in (f). Note that SPP significantly enhanced the density and maturation of vascular structures induced by FGF-2 (arrows). Scale bars in (b), (g), and (h) are 320, 40, and 12.8 μm, respectively. Arrowheads in (A) indicate the border of the matrigel plug.

(B) Quantification of neovessels. Angiogenesis in the fixed matrigel plugs was quantitated by direct counting of vascular structures as described. Data (mean ± SD, n = 4) are from a representative experiment that was repeated twice.

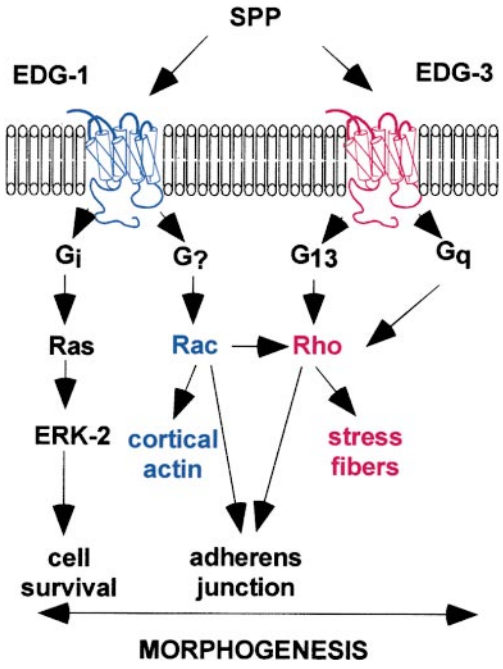

Figure 7. Model of SPP-Induced Morphogenesis in Endothelial Cells

The interaction of G_i with EDG-1 and G_q and G_{13} with EDG-3 has been described (Ancellin and Hla, 1999; Windh et al., 1999). Both G_q and G_{13} are known to induce Rho (Katoh et al., 1998). In contrast, the heterotrimeric G protein responsible for Rac activation is not known. Receptor expression inhibition studies with PTO for EDG-1 and -3 indicate that EDG-1 is required for Rac-coupled cortical actin assembly and EDG-3 is required for Rho-coupled stress fiber formation. Both EDG-1 and EDG-3 are required for adherens junction assembly and endothelial cell morphogenesis, a critical step of angiogenesis.

certain GPCRs may directly bind and activate Rho via the NPxxY motif (Mitchell et al., 1998).

An important question is the requirement for EDG-1 and/or EDG-3 in Rho- and Rac-dependent cytoskeletal changes and adherens junction assembly. Using specific antisense PTOs against EDG-1 and EDG-3, we provide evidence that both receptors are required; namely that EDG-1 regulates Rac-coupled cortical actin formation and EDG-3 regulates Rho-coupled stress fiber formation. Disruption of either pathway by receptor-specific antisense PTO or small GTPase inhibitors (C3 exotoxin and dominant-negative Rac) blocked the SPP-induced adherens junction assembly. The proposed model of SPP signaling in endothelial cells is shown in Figure 7. These data provide novel evidence for the intricate regulation of VE-cadherin function by the extracellular SPP receptors EDG-1 and EDG-3. The dynamic regulation of VE-cadherin function may be critical for vascular system development as well as in the adult; indeed, recent knockout studies of VE-cadherin illustrate the critical role of this molecule in endothelial cell survival and function (Carmeliet et al., 1999).

In addition, SPP protects endothelial cells potently from apoptosis induced by ceramide, 15d-PGJ_2 and growth factor withdrawal. These treatments are known to induce caspase-dependent apoptosis (Cuvillier et al., 1996; Bishop-Bailey and Hla, 1999). SPP was previously shown to protect monocytic cells from ceramide induced apoptosis, which was interpreted to occur via a second messenger action (Cuvillier et al., 1996). In this study, we show that nanomolar concentrations of extracellular SPP prevented endothelial cell apoptosis. This effect was completely blocked by pertussis toxin and the MAP kinase kinase inhibitor PD98059, suggesting that SPP signaling via the G_i pathway is involved. Indeed, antisense PTO for EDG-1 but not EDG-3 attenuated the survival function of SPP. These data imply that SPP may be an important platelet-derived survival factor for endothelial cells.

SPP induced endothelial cell morphogenesis into capillary-like networks in the matrigel model of in vitro angiogenesis. This was potently inhibited by VE-cadherin extracellular domain antibodies, pertussis toxin, and C3 exotoxin. In addition, EDG-1 and EDG-3 antisense PTO attenuated SPP-induced endothelial cell morphogenesis. However, only the EDG-1 antisense PTO attenuated SPP-induced cell survival. These data strongly suggest that the EDG-3 and -1-mediated adherens junction assembly and the protection of endothelial cell survival are required in a coordinated manner during endothelial cell morphogenesis. That EDG-3 antisense PTO alone suppressed SPP-induced morphogenesis strongly suggests that adherens junction assembly is a critical component of morphogenesis. Endothelial cell morphogenesis is a complex process that requires cell–extracellular matrix interactions, directed migration, cell–cell interactions, perivascular proteolysis, and vessel pruning/remodeling, which involves apoptosis. Indeed, inhibition of critical cell–matrix interaction molecules such as $\alpha_v\beta_3$ with antibodies results in endothelial cell apoptosis and vessel regression (Friedlander et al., 1995; Bader et al., 1998). Other studies have also implicated the importance of VE-cadherin in endothelial cell morphogenesis and apoptosis (Bach et al., 1998; Carmeliet et al., 1999). Our data suggest a novel concept that adherens junction assembly is under dynamic control by SPP signaling via EDG-1 and EDG-3 and is required for endothelial cell morphogenesis and survival. This is schematized in Figure 7.

Implantation of SPP- and FGF-2-containing matrigel plugs into athymic mice resulted in significant potentiation of FGF-2-induced angiogenesis. Neovessels formed in the presence of SPP are functionally mature and contain well-developed adherens junctions and basement membranes. However, SPP alone did not induce

(C) Effect of EDG-1 and EDG-3 PTO and VEGF on SPP-induced angiogenesis. αSEDG, antisense EDG-1 (19.2 μM) + antisense EDG-3 (4.8 μM); SEDG, sense EDG-1 (19.2 μM) + sense EDG-3 (4.8 μM). FGF, 1.3 μg/ml; SPP, 500 nM; VEGF, 1.4 μg/ml. (*), FGF + SPP + antisense versus FGF + SPP ($p < 0.05$, t test); (**), VEGF + SPP versus VEGF ($p < 0.05$, t test).

(D) Transmission electron micrographs of SPP-induced neovessels. (a) vehicle; (b) FGF-2; (c) FGF-2 + SPP. Inset shows the higher magnification view of adherens junctional structure between two endothelial cells (arrow in [c]). Arrowheads denote the basement membrane of neovessels (BV) induced by SPP. Nu, nuclei. Scale bars = 5 μm in (a)–(c), and 0.5 μm in the inset.

significant angiogenesis. Thus, mechanistically, SPP likely acts distinctly albeit cooperatively with VEGF, a potent and specific inducer of endothelial cell permeability, survival, and migration (Leung et al., 1989). Vessels formed in the presence of VEGF are leaky and are not functional optimally (Iruela-Arispe and Dvorak, 1997). Indeed, SPP also potentiated VEGF-induced angiogenesis. These data suggest that SPP may be a modulator of angiogenesis which regulates cell–cell junction assembly, morphogenesis, cell survival, and vessel maturation. Endogenous production of SPP by thrombotic platelets and signaling via the EDG-1 pathway may be an important aspect of the angiogenesis process.

Data in this report also imply that activation of the EDG-1 and EDG-3 pathways by SPP agonists may be useful in maximally inducing therapeutic angiogenesis, such as in diabetic wound healing, myocardial angiogenesis after ischemic injury, among others. In addition, combination therapy of SPP-supplemented polypeptide angiogenic factors may be useful in the induction of mature neovessels in vivo. Conversely, inhibition of this pathway by EDG-1 and EDG-3 antagonists may be useful in the inhibition of exaggerated angiogenesis that occurs in various diseases such as solid tumor growth, rheumatoid arthritis, and diabetic retinopathy.

Experimental Procedures

Cell Culture

HUVEC (Clonetics, Cc-2517, p 4–12) were cultured in M199 medium (Mediatech) supplemented with 10% fetal bovine serum (FBS, Hyclone) and heparin-stabilized endothelial cell growth factor, as previously described (Hla and Maciag, 1990). Human embryonic kidney 293 cells (HEK293, ATCC CRL-1573) were cultured in DMEM containing 10% FBS.

Morphogenesis Assay on Matrigel

Morphogenesis on matrigel was performed as described (Passaniti et al., 1992). Briefly, HUVEC were trypsinized, resuspended in plain M199 medium containing soybean trypsin inhibitor (1 mg/ml, Sigma), centrifuged (250 g $\times$ 5 min), resuspended in plain M199 supplemented with 2% charcoal-stripped FBS (CFBS) at a density of 1.5×10^5 cells/ml, and cell suspension (200 μl) was seeded in the presence or absence of SPP (Biomol). Twelve to eighteen hours later, total tubular length was quantitated by image analysis (Gamble et al., 1993).

Poly(A)$^+$ RNA Blot Analysis

Two micrograms of HUVEC and HEK293 poly(A)$^+$ RNA and 280 pg of the EDG-1, EDG-3, EDG-5 in vitro transcripts were loaded and Northern analysis was conducted as described previously (Hla and Maciag, 1990).

Calcium Measurements

Cells were loaded with Indo-1 acetoxymethyl ester (Indo-1/AM, 5 μg/ml; Molecular Probes), for 30 min at 37°C. Intracellular calcium changes were quantitated as described previously (Volpi and Berlin, 1988).

Immunofluorescence Analysis

Cells were plated at 2×10^5 cells in 35 mm glass bottom petri dishes. Two days later, cells were washed and changed to medium M199 supplemented with 10% dialyzed CFBS and growth factors for 16 hr. Subsequently, cells were treated with SPP. After treatment, cells were washed with ice-cold PBS, fixed, and immunofluorescence analysis with various antibodies was conducted as follows: VE-cadherin (1.25 μg/ml, Transduction Labs; 1 μg/ml Santa Cruz), β-catenin (1.25 μg/ml, Transduction Labs), γ-catenin (1.25 μg/ml, Transduction Labs), α-catenin (1.25 μg/ml, Transduction Labs), Tiam1 (1 μg/ml, Santa Cruz), Rac (1 μg/ml, Santa Cruz), Rho (0.4 μg/ml, Santa Cruz). The primary antibody staining was visualized with FITC conjugated goat anti-rabbit or TRITC conjugated sheep anti-mouse (1: 1000, Cappel) IgG. Actin microfilaments were stained with either FTIC- or TRITC-Phalloidin (0.05 μg/ml, Sigma) for 30 min at room temperature. Confocal microscopy analysis was carried out as previously described (Liu et al., 1999).

VE-Cadherin Analysis

HUVEC cells were fractionated with cytoskeleton stabilizing buffer (10 mM HEPES [pH 7.4], 250 mM sucrose, 150 mM KCl, 1 mM EGTA, 3 mM $MgCl_2$, 1$\times$ protease inhibitor cocktail (Calbiochem), 1 mM Na_3VO_4) containing various concentrations of Triton X-100 for 10 min at 4°C (Hinck et al., 1994). Following centrifugation (15,000 $\times$ g, 15 min), the detergent-soluble and -insoluble fractions were separated. The detergent-insoluble fractions were extracted with 1% Triton–1% SDS in cytoskeleton stabilizing buffer at 95°C for 10 min. To detect protein complexes in detergent-insoluble fractions, HUVEC cells were labeled to steady state with [^{35}S]-methionine (250 μCi/ml, NEN DuPont) for 24 hr. After stimulation with 500 nM of SPP for 1 hr, cells were fractionated with 0.5% Triton X-100. After centrifugation (15,000 $\times$ g, 15 min), protein complexes in detergent-insoluble fractions were cross-linked with 0.5 mM DSP (dithiobis[succinimidyl propionate], Pierce) (Hinck et al., 1994), and extracted with 1% Triton X-100–1% SDS as described. Cell extracts were then immunoprecipitated with anti-VE-cadherin, anti-β-catenin, anti-γ-catenin, or anti-p120 Src substrate (p120^{cas}, Transduction). The immunoprecipitated complexes were then released by incubating in sample buffer (20% β-mercaptoethanol) at 95°C for 10 min and addition of 10 μl of 1 M DTT to the gel lanes before protein separation in SDS-PAGE.

Microinjection

HUVEC cells were grown on fibronectin-coated glass bottom dishes for 3 days and microinjected using an Eppendorf Micromanipulator 5171 and Transjector 5246. Approximately 500–800 cells were microinjected cytoplasmically with C3 exoenzyme (0.1 μg/μl, Calbiochem) or dominant-negative N17Rac protein (0.35 μg/μl; Ridley et al., 1992) with Femtotips (Eppendorf) at 100 hPa/0.2 s. Injected cells were marked by coinjecting FITC-rabbit IgG (5 mg/ml, Cappel).

Apoptosis Assay

HUVEC were treated with 1 μM of C_2-ceramide (Biomol) for 12 hr in the presence or absence of SPP. Cells were then fixed with methanol, stained with Hoechst dye (Sigma, 0.5 μg/ml for 5 min). For quantitation, HUVEC cells were labeled with [methyl-^{3}H]-thymidine (5 μCi/ml, NEN DuPont) for 24 hr. Apoptitic DNA was solubilized and quantified as described (Cuvillier et al., 1996).

Angiogenesis In Vivo

Female athymic mice (4–6 weeks old) were injected subcutaneously with 0.4 ml matrigel (approximate protein concentration 9.9 mg/ml, Collaborative Research) premixed with vehicle (fatty acid free BSA, 116 μg/ml, Sigma), FGF-2 (1.3 μg/ml), VEGF (1.4 μg/ml), EDG-1 s/αs PTO (19.2 μM), or EDG-3 s/αs PTO (4.8 μM) in the absence or presence of various concentrations of SPP. Seven days later, matrigel plugs were harvested along with underlying skin and the gross angiogenic response was recorded under a Zeiss Stemi SV6 dissecting microscope (Passaniti et al., 1992). For quantitation, matrigel plugs were fixed with 4% paraformaldehyde in PBS, dehydrated in ethanol and xylene, embedded in paraffin, and sections subjected to hematoxylin and eosin staining. Angiogenesis was quantitated by direct counting of vessels containing red blood cells residing in the stroma interface and the matrigel implant. Each treatment contains 4–5 mice and two random sections from each were quantified. Transmission electron microscopy of 2.5% glutaraldehyde-fixed matrigel plugs was performed as described (Lee et al., 1998).

Phosphothioate Oligonucleotide Treatment

The following 18-mer phosphothioate oligonucleotides (PTO) were synthesized to block the expression of EDG-1 and EDG-3 receptors: antisense EDG-1, 5′-GAC GCT GGT GGG CCC CAT-3′ and 5′-GCT GGT GGG CCC CAT GGT-3′; sense EDG-1, 5′-ATG GGG CCC ACC AGC GTC-3′; scrambled EDG-1, 5′-TGA TCC TTG GCG GGG CCG-3′;

antisense EDG-3, 5′-CGG GAG GGC AGT TGC CAT-3′; sense EDG-3, 5′-ATG GCA ACT GCC CTC CCG-3′; scrambled EDG-3, 5′-ATC CGT CAA GCG GGG GTG-3′; antisense EDG-5, 5′-CGA, GTA CAA GCT GCC CAT-3′. For the antisense EDG-1 PTO, two related sequences whose start points differ by 3 bases were used. Both sequences exhibited similar inhibition of EDG-1 expression and biological effects in HUVEC. The specificity and efficacy of the PTOs were tested in *Xenopus* oocytes programmed to express EDG-1 and -3 receptors (Ancellin and Hla, 1999). Briefly, oocytes were injected with 20 nl of capped messenger RNA (EDG-1 + Gqi chimeric G protein, 1 μg/ml of each; EDG-3, 50 ng/ml) premixed with the indicated PTO (100 ng/μl in water). Thirty-two hours after injection, oocytes were injected with photoprotein Aequorin (20 nl of 1 mg/ml) and stimulated with 20 nM of SPP. Light emission was recorded for 90 s with a luminometer (Turner Design). Each experiment was repeated at least three times with multiple oocytes from different frogs. To examine the effects on HUVEC, PTOs and FITC-IgG were microinjected into the cytoplasm of HUVEC cells using the Eppendorf Transjector microinjector system as described (Macrez-Lepretre et al., 1997). Alternatively, PTOs were delivered into HUVEC by Lipofectin reagent (Life Technologies, Inc.), essentially as described (Ackermann et al., 1999).

Supplemental Data

For additional data dealing with actin cytoskeletal changes, β-catenin translocation, intracellular microinjection of SPP, and pertussis toxin effects, which could not be presented here due to space limitations, see http://www.cell.com/cgi/content/full/99/3/301/DC1.

Acknowledgments

We thank Dr. Alan Hall for the generous gift of the dominant-negative Rac construct, Dr. Harold Benjamin for recombinant bFGF, Dr. Arthur Hand and Ms. Christine Pearson for expert EM help, Ms. Christine Jozef for expert secretarial help, Dr. Anshu Agarwal and Mr. Sung-Suk Chae for technical help, and Dr. James Watras for the help with calcium measurements. This work is supported by NIH grants (DK45659 and HL54710 to T. H.; CA64436 to K. P. C.). T. H. is an established investigator of the American Heart Association.

Received May 14, 1999; revised September 20, 1999.

References

Ackermann, E.J., Taylor, J.K., Narayana, R., and Bennett, C.F. (1999). The role of antiapoptotic Bcl-2 family members in endothelial apoptosis elucidated with antisense oligonucleotides. J. Biol. Chem. *274*, 11245–11252.

An, S., Bleu, T., Hallmark, O.G., and Goetzl, E.J. (1998). Characterization of a novel subtype of human G protein–coupled receptor for lysophosphatidic acid. J. Biol. Chem. *273*, 7906–7910.

Ancellin, N., and Hla, T. (1999). Differential pharmacological properties and signal transduction of sphingosine-1-phosphate receptors EDG-1, EDG-3 and EDG-5. J. Biol. Chem. *274*, 18997–19002.

Bach, T.L., Barsigian, C., Chalupowicz, D.G., Busler, D., Yaen, C.H., Grant, D.S., and Martinez, J. (1998). VE-Cadherin mediates endothelial cell capillary tube formation in fibrin and collagen gels. Exp. Cell Res. *238*, 324–334.

Bader, B.L., Rayburn, H., Crowley, D., and Hynes, R.O. (1998). Extensive vasculogenesis, angiogenesis, and organogenesis precede lethality in mice lacking all alpha v integrins. Cell *95*, 507–519.

Bishop-Bailey, D., and Hla, T. (1999). Endothelial cell apoptosis induced by peroxisomal proliferator activator-γ ligand 15-deoxy-$\Delta^{12,14}$ prostaglandin J_2. J. Biol. Chem. *274*, 17042–17048.

Braga, V.M., Machesky, L.M., Hall, A., and Hotchin, N.A. (1997). The small GTPases Rho and Rac are required for the establishment of cadherin-dependent cell–cell contacts. J. Cell Biol. *137*, 1421–1431.

Carmeliet P., Lampugnani, M.G., Moons, L., Breviario, F., Compernolle, V., Bono, F., Balconi, G., Spagnuolo, R., Oosthuyse, B., Dewerchin, M., et al. (1999). Targeted deficiency or cytosolic truncation of the VE-cadherin gene in mice impairs VEGF-mediated endothelial survival and angiogenesis. Cell *98*, 147–157.

Cuvillier, O., Pirianov, G., Kleuser, B., Vanek, P.G., Coso, O.A., Gutkind, S., and Spiegel, S. (1996). Suppression of ceramide-mediated programmed cell death by sphingosine-1-phosphate. Nature *381*, 800–803.

Eliceiri, B.P., and Cheresh, D.A. (1999). The role of alpha v integrins during angiogenesis: insights into potential mechanisms of action and clinical development. J Clin. Invest. *103*, 1227–1230.

Esser, S., Lampugnani, M.G., Corada, M., Dejana, E., and Risau, W. (1998). Vascular endothelial growth factor induces VE-cadherin tyrosine phosphorylation in endothelial cells. J. Cell Sci. *111*, 1853–1865.

Exton, J.H. (1997). Cell signaling through guanine-nucleotide-binding regulatory proteins (G proteins) and phospholipases. Eur. J. Biochem. *243*, 10–20.

Folkman, J. (1995). Angiogenesis in cancer, vascular, rheumatoid and other disease. Nat. Med. *1*, 27–31.

Folkman, J., and Haudenschild, C. (1980). Angiogenesis in vitro. Nature *288*, 551–556.

Friedlander, M., Brooks, P.C., Shaffer, R.W., Kincaid, C.M., Varner, J.A., and Cheresh, D.A. (1995). Definition of two angiogenic pathways by distinct alpha v integrins. Science *270*, 1500–1502.

Friesel, R.E., and Maciag, T. (1995). Molecular mechanisms of angiogenesis: fibroblast growth factor signal transduction. FASEB J. *9*, 919–925.

Gamble, J.R., Matthias, L.J., Meyer, G., Kaur, P., Russ, G., Faull, R., Berndt, M.C., and Vadas, M.A. (1993). Regulation of in vitro capillary tube formation by anti-integrin antibodies. J. Cell Biol. *121*, 931–943.

Hall, A. (1998). Rho GTPases and the actin cytoskeleton. Science *279*, 509–514.

Hecht, J.H., Weiner, J.A., Post, S.R., and Chun, J. (1996). Ventricular zone gene-1 (vzg-1) encodes a lysophosphatidic acid receptor expressed in neurogenic regions of the developing cerebral cortex. J. Cell Biol. *135*, 1071–1083.

Hinck, L., Nathke, I.S., Papkoff, J., and Nelson, W.J. (1994). Dynamics of cadherin/catenin complex formation: novel protein interactions and pathways of complex assembly. J. Cell Biol. *125*, 1327–1340.

Hla, T., and Maciag, T. (1990). An abundant transcript induced in differentiating human endothelial cells encodes a polypeptide with structural similarities to G-protein-coupled receptors. J. Biol. Chem. *265*, 9308–9313.

Hla, T., Lee, M., Ancellin, N., Liu, C.H., Thangada, S., Thompson, B.D., and Kluk, M. (1999). Sphingosine-1-phosphate: extracellular mediator or intracellular second messenger? Biochem. Pharm. *58*, 201–207.

Ilan, N., Mahooti, S., and Madri, J.A. (1998). Distinct signal transduction pathways are utilized during the tube formation and survival phases of in vitro angiogenesis. J. Cell Sci. *111*, 3621–3631.

Iruela-Arispe, M.L., and Dvorak, H.F. (1997). Angiogenesis: a dynamic balance of stimulators and inhibitors. Thromb. Haemost. *78*, 672–677.

Katoh, H., Aoki, J., Yamaguchi, Y., Kitano, Y., Ichikawa, A., and Negishi, M. (1998). Constitutively active Galpha12, Galpha13, and Galphaq induce Rho-dependent neurite retraction through different signaling pathways. J. Biol. Chem. *273*, 28700–28707.

Lee, M.J., Evans, M., and Hla, T. (1996). The inducible G protein–coupled receptor edg-1 signals via the G(i)/mitogen-activated protein kinase pathway. J. Biol. Chem. *271*, 11272–11279.

Lee, M.J., Van Brocklyn, J.R., Thangada, S., Liu, C.H., Hand, A.R., Menzeleev, R., Spiegel, S., and Hla, T. (1998). Sphingosine-1-phosphate as a ligand for the G protein–coupled receptor EDG-1. Science *279*, 1552–1555.

Leung, D.W., Cachianes, G., Kuang, W.J., Goeddel, D.V., and Ferrara, N. (1989). Vascular endothelial growth factor is a secreted angiogenic mitogen. Science *246*, 1306–1309.

Liu, C.H., and Hla, T. (1997). The mouse gene for the inducible G-protein-coupled receptor edg-1. Genomics *43*, 15–24.

Liu, C.H., Thangada, S., Lee, M.J., Van Brocklyn, J.R., Spiegel, S., and Hla, T. (1999). Ligand-induced trafficking of the sphingosine-1-phosphate receptor EDG-1. Mol. Biol. Cell *10*, 1179–1190.

Macrez-Lepretre, N., Kalkbrenner, F., Morel, J.L., Schultz, G., and Mironneau, J. (1997). G protein heterotrimer Galpha13beta1gamma3 couples the angiotensin AT1A receptor to increases in cytoplasmic Ca^{2+} in rat portal vein myocytes. J. Biol. Chem. *272*, 10095–10102.

Michiels, F., Habets, G.G., Stam, J.C., van der Kammen, R.A., and Collard, J.G. (1995). A role for Rac in Tiam1-induced membrane ruffling and invasion. Nature *375*, 338–340.

Mitchell, R., McCullough, D., Lutz, E., Johnson, M., MacKenzie, C., Fennell, M., Fink, G., Zhou, W., and Sealfon, S.C. (1998). Rhodopsin-family receptors associate with small G proteins to activate phospholipase D. Nature *392*, 411–414.

Montesano, R., and Orci, L. (1985). Tumor-promoting phorbol esters induce angiogenesis in vitro. Cell *42*, 469–477.

Nobes, C.D., and Hall, A. (1995). Rho, rac, and cdc42 GTPases regulate the assembly of multimolecular focal complexes associated with actin stress fibers, lamellipodia, and filopodia. Cell *81*, 53–62.

Okazaki, H., Ishizaka, N., Sakurai, T., Kurokawa, K., Goto, K., Kumada, M., and Takuwa, Y. (1993). Molecular cloning of a novel putative G protein–coupled receptor expressed in the cardiovascular system. Biochem. Biophys. Res. Commun. *190*, 1104–1109.

O'Reilly, M.S., Boehm, T., Shing, Y., Fukai, N., Vasios, G., Lane, W.S., Flynn, E., Birkhead, J.R., Olsen, B.R., and Folkman, J. (1997). Endostatin: an endogenous inhibitor of angiogenesis and tumor growth. Cell *88*, 277–285.

Passaniti, A., Taylor, R.M., Pili, R., Guo, Y., Long, P.V., Haney, J.A., Pauly, R.R., Grant, D.S., and Martin, G.R. (1992). A simple, quantitative method for assessing angiogenesis and antiangiogenic agents using reconstituted basement membrane, heparin, and fibroblast growth factor. Lab. Invest. *67*, 519–528.

Postma, F.R., Jalink, K., Hengeveld, T., and Moolenaar, W.H. (1996). Sphingosine-1-phosphate rapidly induces Rho-dependent neurite retraction: action through a specific cell surface receptor. EMBO J. *15*, 2388–2392.

Ridley, A.J., Paterson, H.F., Johnston, C.L., Diekmann, D., and Hall, A. (1992). The small GTP-binding protein rac regulates growth factor-induced membrane ruffling. Cell *70*, 401–410.

Satake, S., Kuzuya, M., Ramos, M.A., Kanda, S., and Iguchi, A. (1998). Angiogenic stimuli are essential for survival of vascular endothelial cells in three-dimensional collagen lattice. Biochem. Biophys. Res. Commun. *244*, 642–646.

Spiegel, S., and Merril, A.H., Jr. (1996). Sphingolipid metabolism and cell growth regulation. FASEB J. *10*, 1388–1397.

Takaishi, K., Sasaki, T., Kotani, H., Nishioka, H., and Takai, Y. (1997). Regulation of cell–cell adhesion by Rac and Rho small G proteins in MDCK cells. J. Cell Biol. *139*, 1047–1059.

Volpi, M., and Berlin, R.D. (1988). Intracellular elevation of free calcium induced by activation of histamine H1 receptors in interphase and mitotic Hela cells: homone signal transduction is altered during mitosis. J. Cell Biol. *107*, 2533–2539.

Windh, R.T., Lee, M-J., Hla, T., An, S., Barr, A.J., and Manning, D.R. (1999). Differential coupling of the sphingosine 1-phosphate receptors Edg-1, Edg-3 and H218/Edg-5 to the G_z, G_q and G_{12} families of heterotrimeric G proteins. J. Biol. Chem. *274*, 27351–27357.

Wojciak-Stothard, B., Entwistle, A., Garg, R., and Ridley, A.J. (1998). Regulation of TNF-α induced reorganization of the actin cytoskeleton and cell–cell junctions by Rho, Rac and Cdc42 in human endothelial cells. J. Cell. Physiol. *176*, 150–165.

Yamaguchi, F., Tokuda, M., Hatase, O., and Brenner, S. (1996). Molecular cloning of the novel human G protein–coupled receptor (GPCR) gene mapped on chromosome 9. Biochem. Biophys. Res. Commun. *227*, 608–614.

Yap, A.S., Brieher, W.M., and Gumbiner, B.M. (1997). Molecular and functional analysis of cadherin-based adherens junctions. Annu. Rev. Cell Dev. Biol. *13*, 119–146.

Yatomi, Y., Igarashi, Y., Yang, L., Hisano, N., Qi, R., Asazuma, N., Satoh, K., Ozaki, Y., and Kume, S. (1997). Sphingosine 1-phosphate, a bioactive sphingolipid abundantly stored in platelets, is a normal constituent of human plasma and serum. J. Biochem. (Tokyo), *12*, 969–973.